2008 American Control Conference
Westin Seattle Hotel, Seattle, Washington, USA
June 11-13, 2008

Modeling and Control of a Two Stroke HCCI Engine

Maxim V. Subbotin, Karl Lukas Knierim, Sungbae Park, Aleksandar Kojic, Jasim Ahmed

Abstract— **In this paper we propose a model of a two stroke Homogeneous Charge Compression Ignition (HCCI) engine which captures the important characteristics of gas exchange processes taking place in a two stroke mode. The model allows a direct flow of gases between intake and exhaust volumes and hence offers a more detailed gas modeling than single volume models widely accepted in the literature. We compare simulation results obtained from the model with experimental data collected with a single cylinder HCCI engine. We also propose a simple control strategy allowing effective tracking of reference signals in Indicated Mean Effective Pressure (IMEP) and combustion phasing.**

I. Introduction

Homogeneous Charge Compression Ignition technology has received a lot of attention during the past few years due to the potential to reduce emissions while increasing fuel economy. Reduction of emissions in Nitrous Oxides (NO_x) is a consequence of much lower combustion temperatures in HCCI engines in comparison to conventional spark ignition (SI) and diesel engines [12]. Lower emissions in Carbon Monoxide (CO) and improved fuel economy are explained by a high dilution of charge and low throttling loses in HCCI engines [13], [5].

A great challenge in achieving HCCI regime comes from the fact that unlike in SI or diesel engines where combustion is initiated with a spark or by fuel injection, respectively, HCCI lacks a specific event initiating combustion. To harvest all plausible characteristics of the HCCI combustion it is necessary to employ an active control system which can initiate and control the combustion process. The combustion process in HCCI regime is governed by chemical kinetics of mixture of fuel, reinducted or trapped exhaust gases and fresh charge. To analyze the processes taking place in the HCCI engine and synthesize a control system we need a model of the system which can capture important behavioral characteristics. There are several modeling methods presented in the literature. Some of these methods, mostly those oriented on modeling for analysis, describe the combustion processes in great detail and are applicable to HCCI engines working in different regimes. Just to mention a few, multi-zone models [5], [16] describe nonuniform temperature distribution of gases inside a cylinder, other methods include stochastic and multi-dimensional CFD models [11], [2], [1]. Another group of modeling methods is oriented on modeling for control. These methods include low order cycle-to-cycle discrete models [18], [3] trying to capture an evolution of characteristic variables necessary for control implementation. Another alternative is a relatively simple continuous time single-zone models based on physical principles which showed to be very effective in describing behavior of the states of the engine [17], [8]. The models of the latter group are considering specific control inputs applied to the system and, as a consequence, are developed for a particular mode of the HCCI engine, a four stroke HCCI mode.

A two stroke HCCI mode proposes an interesting alternative to a four stroke mode, while this area of HCCI modeling remains undeveloped. In this paper we propose a continuous time, physics based model which describes important gas exchange processes taking place in the two stroke HCCI mode, not captured in the four stroke models presented in the literature. The main difference of the proposed model is an introduction of a direct gas flow between intake and exhaust volumes. Direct flow of gases is taking place in the two stroke mode due to valve overlap and should not be neglected in modeling because of its significant effect on the system state. In order to define mass flows in the engine we introduce intake and exhaust volumes in addition to a cylinder volume and define concentrations of important species in these volumes. Due to the explicit modeling of the species in the intake and the exhaust the proposed model naturally captures cycle-to-cycle coupling of the physical processes taking place in the engine. As a result it can be used for the synthesis of control systems employing various methods to control the HCCI process, which may include reinducting or trapping combustion products from previous cycle [17], [18], [4] and heating or precompressing the intake charge [14], [20]. For the prediction of the combustion timing we use a well-established integrated Arrhenius threshold method, while the combustion is modeled with a Wiebe function [17], [10], [6].

To validate the proposed model we compare simulation results obtained from the model with an experimental data collected from a single cylinder engine. For the comparison of the behavior within one cycle we use in-cylinder pressure traces. For the comparison in different operating conditions we use IMEP [19] values and the amount of air flow. Based on the behavior of the engine observed during the experiments and in simulation we propose a control strategy which can effectively control IMEP and combustion phasing of the two stroke engine. Our control strategy is essentially an implementation of the methods regulating proportion of a fresh charge and exhaust gases trapped in the cylinder to control HCCI combustion.

M. V. Subbotin, Department of Electrical and Computer Engineering, University of California, Santa Barbara, CA 93106-9560, USA, subbotin@engineering.ucsb.edu, K. L. Knierim, S. Park, A. Kojic, and J. Ahmed, RTC-EMCC, Robert Bosch LLC, (karl.knierim,sungbae.park,aleksandar.kojic, jasim.ahmed)@us.bosch.com

II. HCCI MODELING

We base our modeling approach on the first law of thermodynamics for an open system. To model the mass flows between volumes we use steady state compressible flow relations. In order to capture the gas and chemistry dynamics of the two stroke HCCI engine during one complete engine cycle, we introduce 19 dynamic states describing temperatures and concentrations of the main gas species in the cylinder, intake and exhaust volumes, and the crank angle. While the cylinder volume, V_c, is a well defined quantity for an internal combustion engine, the intake, V_i, and exhaust, V_e, volumes introduced in our model are fictitious parameters. In our model we assign these parameters to the approximate volumes of intake and exhaust manifolds respectively.

We define the following states for the system model. Intake volume: the intake volume temperature, T_i; the concentrations of fuel, X_i^f, oxygen, $X_i^{O_2}$, nitrogen, $X_i^{N_2}$, carbon dioxide, $X_i^{CO_2}$, and water, $X_i^{H_2O}$. Exhaust volume: the exhaust volume temperature, T_e; the concentrations of fuel, X_e^f, oxygen, $X_e^{O_2}$, nitrogen, $X_e^{N_2}$, carbon dioxide, $X_e^{CO_2}$, and water, $X_e^{H_2O}$. Cylinder: the crank angle, θ; the temperature, T_c; the concentrations of fuel, X_c^f, oxygen, $X_c^{O_2}$, nitrogen, $X_c^{N_2}$, carbon dioxide, $X_c^{CO_2}$, and water, $X_c^{H_2O}$.

With the crank angle calculated from,

$$\dot{\theta} = \omega, \tag{1}$$

the volume of the cylinder for any instant of time can be calculated from a well know slider-crank formula [6]:

$$V = V_c + \frac{\pi B^2}{4}(l + a - a \cdot \cos\theta - \sqrt{l^2 - a^2 \sin^2\theta}), \tag{2}$$

where ω is the crankshaft speed, a is equal to half of the length of the stroke, l is the length of the connecting rod, B is the bore diameter, and V_c is the clearance volume at the top dead center.

To be able to derive differential equations for the concentrations of species, we have to define masses and mass flows between model volumes. There are eight mass flows introduced in the model, see Figure 1. These allow accounting for the gas exchange between the intake and the exhaust volumes and the cylinder, as well as direct flows between the intake and the exhaust. Possible mass flows through the intake valve are a flow from the intake volume to the cylinder, $\dot{m}_{ic}$, back flow from the cylinder to the intake volume, $\dot{m}_{ci}$, and two direct flows between the intake and the exhaust, a flow from the intake to the exhaust, $\dot{m}_{ie}$, and from the exhaust to the intake, $\dot{m}_{ei}$. Analogously mass flows through the exhaust valve are a flow from the cylinder to the exhaust volume, $\dot{m}_{ce}$, back flow from the exhaust to the cylinder, $\dot{m}_{ec}$, and the flows $\dot{m}_{ie}$, $\dot{m}_{ei}$.

To model each of the mass flows we use equations for a steady-state compressible isentropic flow analysis [6]. For a choked flow,

$$\dot{m} = \frac{C_D A_T p_0}{\sqrt{RT_0}} \sqrt{\gamma} \left(\frac{2}{\gamma+1}\right)^{(\gamma+1)/2(\gamma-1)},$$

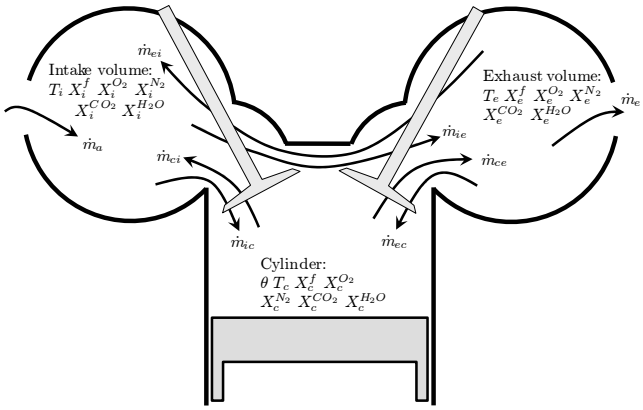

Fig. 1. Intake volume, cylinder, and exhaust volume with mass flows and system states.

when $p_T/p_0 \leq (2/(\gamma+1))^{\gamma/(\gamma-1)}$. And for a subsonic flow,

$$\dot{m} = \frac{C_D A_T p_0 p_T^{\frac{1}{\gamma}}}{\sqrt{RT_0} p_0^{\frac{1}{\gamma}}} \sqrt{\frac{2\gamma}{\gamma-1}\left(1 - \left(\frac{p_T}{p_0}\right)^{\frac{\gamma-1}{\gamma}}\right)},$$

when $p_T/p_0 > (2/(\gamma+1))^{\gamma/(\gamma-1)}$. Here p_0 and T_0 are the upstream stagnation pressure and temperature respectively, p_T is the downstream pressure, and γ is the specific heat ratio. A_T is an opening area and C_D is a discharge coefficient which accounts for a difference between ideal and real gas flows.

The opening area, A_T, for each flow is defined in the following way. First, we find the minimum between current valve opening areas, $A_{min} = \min(A_i, A_e)$, where A_i is the opening area of the intake valve, and A_e is the opening area of the exhaust valve. Now using A_{min}, we define $A_d = kA_{min}$ - an area of the opening utilized by the direct flow between the intake and the exhaust volumes. Coefficient $k \in (0, 1)$ defines a percentage of total opening area used by a direct flow. Once A_d is found, we calculate $A_{ic} = A_i - A_d$ - a portion of the intake valve opening area used by the flows between the intake and the cylinder, and $A_{ec} = A_e - A_d$ - a portion of the exhaust valve opening area used by the flows between the exhaust and the cylinder.

Using values of pressures in the intake and exhaust volumes and the cylinder, we calculate possible direct flows between the intake and the exhaust volumes when both valves are opened simultaneously. If $p_i > p_c$ and $p_i > p_e$ we allow for a positive flow from the intake volume into the exhaust volume, $\dot{m}_{ie} \geq 0$, $\dot{m}_{ei} = 0$. If $p_e > p_c$ and $p_e > p_i$ then $\dot{m}_{ei} \geq 0$, $\dot{m}_{ie} = 0$. Similar logic is used for the calculation of flows between the intake and the exhaust volumes and the cylinder, if the pressure in one volume is greater than the other, we allow for the positive flow from the first volume to the second and the opposite flow is zero.

A. Concentrations

With a well defined mass flows between volumes of the model we can derive equations for the rates of

change of concentrations of different species in these volumes. The rate of change of species' concentrations $s \in \{f, O_2, N_2, CO_2, H_2\}$, $\dot{X}_i^s$, $\dot{X}_e^s$, in the intake, V_i, and exhaust, V_e, volumes respectively are defined as,

$$\begin{aligned} \dot{X}_i^s &= \dot{N}_i^s / V_i, \\ \dot{X}_e^s &= \dot{N}_e^s / V_e, \end{aligned} \tag{3}$$

where N_i^s and N_e^s are the number of moles of species s in the intake and exhaust volumes respectively. The rates of change of moles of species s per unit volume are related to the mass flows in the following way [17],

$$\begin{aligned} \frac{\dot{N}_i^s}{V_i} &= \frac{Y_a^s \dot{m}_a + Y_c^s \dot{m}_{ci} + Y_e^s \dot{m}_{ei} - Y_i^s \dot{m}_{ic} - Y_i^s \dot{m}_{ie}}{V_i M W^s}, \\ \frac{\dot{N}_e^s}{V_e} &= \frac{Y_c^s \dot{m}_{ce} + Y_i^s \dot{m}_{ie} - Y_e^s \dot{m}_{ec} - Y_e^s \dot{m}_{ei} - Y_e^s \dot{m}_e}{V_e M W^s}, \end{aligned} \tag{4}$$

where Y_a^s, Y_i^s, Y_e^s, Y_c^s are the mass fractions of species s in the atmosphere, the intake, the exhaust volumes, and the cylinder respectively, and MW^s is the specie's molecular mass. While Y_a^s is assumed to be constant, Y_i^s, Y_e^s, and Y_c^s vary during engine cycle and can be found from,

$$\begin{aligned} Y_i^s &= \frac{X_i^s MW^s}{\sum_s X_i^s MW^s}, \\ Y_e^s &= \frac{X_e^s MW^s}{\sum_s X_e^s MW^s}, \\ Y_c^s &= \frac{X_c^s MW^s}{\sum_s X_c^s MW^s}. \end{aligned} \tag{5}$$

For the concentrations of species inside the cylinder volume we can write,

$$\dot{X}_c^s = \frac{\dot{N}_c^s}{V} - \frac{\dot{V} N^s}{V^2} = \frac{\dot{N}_c^s}{V} - \frac{\dot{V} X_c^s}{V}, \tag{6}$$

where $\dot{V}$ can be found by differentiating (2),

$$\dot{V} = \frac{\pi B^2 a \dot{\theta} \sin\theta}{4} \left(1 + \frac{a \cos\theta}{\sqrt{l^2 - a^2 \sin^2\theta}} \right). \tag{7}$$

For the cylinder volume the rate of change of moles of species per unit volume is defined by the mass flows between the cylinder and the intake and the exhaust volumes and by the combustion reactions inside the cylinder.

$$\frac{\dot{N}_c^s}{V} = \omega_c^s + \frac{Y_i^s \dot{m}_{ic} + Y_e^s \dot{m}_{ec} - Y_c^s \dot{m}_{ci} - Y_c^s \dot{m}_{ce}}{V M W^s}, \tag{8}$$

where ω_c^s is a combustion reaction rate defined with a combustion model. To predict the combustion phasing and evolution we use the integrated Arrhenius rate threshold method [17].

B. Temperature Rates

We use first law of thermodynamics for an open system in combination with the ideal gas law to derive a differential equations for the rates of changes of temperatures inside the intake and exhaust volumes and the cylinder [6], [17]. The difference between two volumes and the cylinder is that there is no work produced in the intake and the exhaust volumes. The first law of thermodynamics written for the cylinder gives,

$$\frac{d(m_c u_c)}{dt} = \dot{Q}_c - \dot{W}_c + \dot{M}_c, \tag{9}$$

where m_c is the mass of species in the cylinder and u_c is the internal energy of the cylinder contents, and $\dot{M}_c \equiv \dot{m}_{ic} h_i + \dot{m}_{ec} h_e - \dot{m}_{ci} h_c - \dot{m}_{ce} h_c$. The convective heat transfer to the walls of the cylinder is modeled with,

$$\dot{Q}_c = -\bar{h}_c A_w (T_c - T_{wall}), \tag{10}$$

here A_w is the surface area of the cylinder walls, T_{wall} is the average cylinder wall temperature, and $\bar{h}_c$ is the convection coefficient found with a Woshni heat transfer model [10]. $\dot{W}_c = p_c \dot{V}$ is the work output rate. h_i, h_e, and h_c are the enthalpies of species in the intake volume, the exhaust volume and the cylinder respectively. We can express enthalpy in terms of internal energy, $h_c = u_c + p_c V / m_c$. Rearranging and taking the derivative we arrive at,

$$\frac{d(m_c h_c)}{dt} = \frac{d(m_c u_c)}{dt} + \dot{p}_c V + p_c \dot{V}. \tag{11}$$

Now combining (9) and (11), we achieve,

$$\frac{d(m_c h_c)}{dt} = \dot{Q}_c + \dot{p}_c V + \dot{M}_c. \tag{12}$$

We can also approach the relation for enthalpy from another direction,

$$m_c h_c = \sum_s N_c^s \hat{h}_c^s, \tag{13}$$

where $\hat{h}_c^s$ is the molar enthalpy of species s in the cylinder. Taking the derivative we arrive at,

$$\frac{d(m_c h_c)}{dt} = \sum_s \dot{N}_c^s \hat{h}_c^s + \sum_s N_c^s \dot{\hat{h}}_c^s. \tag{14}$$

With the expression for the rate of change of enthalpy per unit mole of species s, $\dot{\hat{h}}_c^s = C^s(T_c) \dot{T}_c$, where $C^s(T_c)$ is the constant pressure specific heat of species s per mole at temperature T_c, and noting that $\dot{N}^s = \dot{X}^s V + \dot{V} X^s$ we can rewrite (14) as,

$$\frac{d(m_c h_c)}{dt} = V \sum_s \dot{X}_c^s \hat{h}_c^s + \dot{V} \sum_s X_c^s \hat{h}_c^s + \dot{T}_c V \sum_s X_c^s C^s(T_c). \tag{15}$$

Now we can use the ideal gas law, $p_c = \sum_s X_c^s R T_c$, and take a derivative, $\dot{p}_c = R T_c \sum_s \dot{X}_c^s + R \dot{T}_c \sum_s X_c^s$ to substitute into equation (12). At this point we can equate right sides of equations (12) and (14) and express the rate of change of the temperature,

$$\dot{T}_c = \frac{\dot{Q}_c + V \sum_s \dot{X}_c^s (R T_c - \hat{h}_c^s) - \dot{V} \sum_s X_c^s \hat{h}_c^s + \dot{M}_c}{V \sum_s X_c^s (C^s(T_c) - R)}. \tag{16}$$

Following similar steps we derive differential equations for the temperatures of the intake and the exhaust volumes,

$$\begin{aligned} \dot{T}_i &= \frac{\dot{Q}_i + V_i R T_i \sum_s \dot{X}_i^s - V_i \sum_s \dot{X}_i^s \hat{h}_i^s + \dot{M}_i}{V_i \sum_s X_i^s (C^s(T_i) - R)}, \\ \dot{T}_e &= \frac{\dot{Q}_e + V_e R T_e \sum_s \dot{X}_e^s - V_e \sum_s \dot{X}_e^s \hat{h}_e^s + \dot{M}_e}{V_e \sum_s X_e^s (C^s(T_e) - R)}, \end{aligned} \tag{17}$$

where $\dot{M}_i \equiv \dot{m}_a h_a + \dot{m}_{ci} h_c + \dot{m}_{ei} h_e - \dot{m}_{ic} h_i - \dot{m}_{ie} h_i$ and $\dot{M}_e \equiv \dot{m}_{ce} h_c + \dot{m}_{ie} h_i - \dot{m}_{ec} h_e - \dot{m}_{ei} h_e - \dot{m}_e h_e$. Equations (1), (3)-(8), and (16)-(17) describe the dynamics of the proposed model.

C. Simulation Results

Using the described system model we run a series of simulations to observe the behavior of the engine in various points of operation. For all the simulation results presented in this paper we used $k = 0.25$ for the percentage of the direct flow between volumes. Isooctane was used as a fuel.

Figure 2 shows temperature and pressure traces for the intake, the exhaust volume, and the cylinder for one of the operating points of the engine. Valve opening and closing instants as well as the fuel injection period are also indicated on the figure to give a better insight into the processes taking place in the volumes and the cylinder. We used the following settings for the simulation experiment represented on Figure 2: $IVO = 165[deg]$, $IVC = -90[deg]$, $EVO = 120[deg]$, $EVC = -140[deg]$, $fuel = 9[mg]$. Let's take a closer look at the evolution of the pressure and temperature in one of the model volumes, the intake volume. The new cycle starts at -180 $[deg]$ from the Top Dead Center (TDC) when both intake and exhaust valve are open. Both the temperature and the pressure in the intake volume grow slowly until EVC due to piston pumping which pushes some of the hot charge from the cylinder back into the intake volume. After EVC the temperature and the pressure grow fast until IVC, because the hot charge can move only into the intake volume. After IVC the temperature and the pressure decrease slowly as the gases in the intake volume cool down. After IVO the temperature and the pressure drop rapidly down due to the fast flow though the intake volume into the cylinder and the exhaust volume. Similar processes are happening in the exhaust volume. Processes in the cylinder are influenced by the fuel injection and the combustion process in addition to the gas and temperature exchanges in the intake the exhaust volumes.

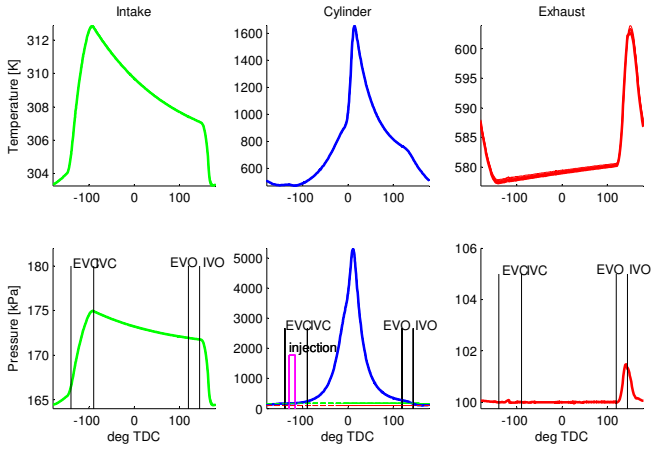

Fig. 2. Temperature and pressure traces for the intake volume, the cylinder, and the exhaust volume.

III. Comparison with Experimental Data

To validate the proposed model, we compare simulation data achieved with the model and the data available from experiments. The experimental data was collected on a single cylinder HCCI engine with a variable valve actuation system [17], [18]. Both experiments and simulations showed that IVO and the amount of injected fuel can be used very effectively to control the HCCI engine working in the two-stroke regime. Hence other input variables, IVC, EVO, EVC, and injection timing, were fixed in all the experiments and simulations described below. The values used in experiments and simulations were set to: $IVC = -90$ $[deg]$, $EVO = 120$ $[deg]$, $EVC = -140$ $[deg]$, injection instant $= -130$ $[deg]$.

One of the variables available for the measurements during the operation of the experimental system is a cylinder pressure, p_c. Figure (3) and Figure (4) show pressure traces recorded during the experiments together with the simulation results for two operating points of the engine. Figure (4) shows the traces for the operating point with input settings $IVO = 140$ $[deg]$, $fuel = 14.4$ $[mg]$, and Figure (3) shows the results for the operating point with the input values $IVO = 165$ $[deg]$, $fuel = 9$ $[mg]$. The simulation and experimental curves show a good fit on average. Significant variations in experimental pressure traces around the combustion interval are natural for uncontrolled HCCI engines especially those working in a two-stroke mode. The differences between simulation results and experimental traces on the combustion and expansion intervals are due to the errors in the combustion model. Most importantly for validation of the proposed model, the pressure traces show a very good fit on the interval where the gas exchange processes are taking place in the system.

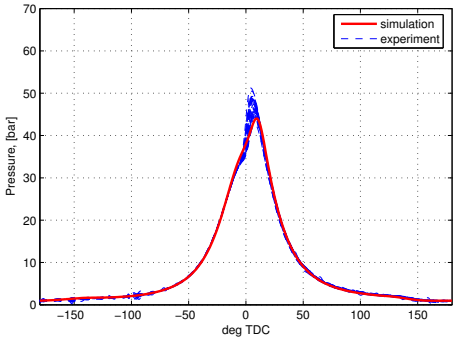

Fig. 3. Experimental and simulated pressure traces for $IVO = 165[deg]$, $fuel = 9[mg]$.

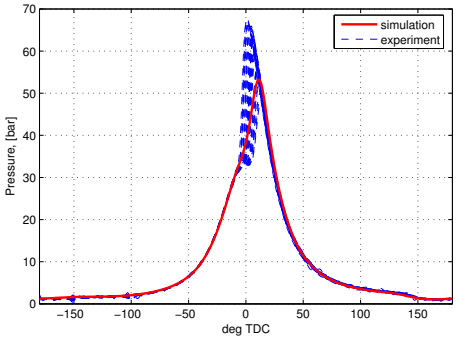

Fig. 4. Experimental and simulated pressure traces for $IVO = 140[deg]$, $fuel = 14.4[mg]$.

To compare the simulation model with the experimental system in different operating points, we calculated the values of $IMEP$ and air flow for the range of input values. This comparison is especially important for the model based controller design as it should show if the model captures the influence of the system inputs on the system outputs.

Figures 5 and 6 show relationship between $IMEP$ and the combined input in IVO and the amount of fuel which were adjusted simultaneously. Figure 7 shows the relationship between average air flow through the cylinder and IVO. Offsets in the simulated and experimental $IMEP$ and an offset in the amount of fresh air passed through the cylinder show a discrepancy between the model and the experimental system. A greater efficiency of the model can be explained by some real phenomena not accounted for in the modeling process. In addition to that the experimental system displays significant oscillations in pressure traces from cycle to cycle which should also result in lower efficiency. An approximate heat exchange model used in the modeling process may as well contribute to the seemingly higher efficiency of the model and requires its own verification. We did not make any effort in tuning parameters of the model to match simulation results with the experimental data though the proposed model offers great flexibility. The most important observation for the verification of the proposed model and for the future model-based controller design is the fact that the slopes of the curves of Figures 5-7 are almost identical. This indicates that the experimental system and the proposed model react similarly on variations of the control inputs, IVO and the amount of injected fuel.

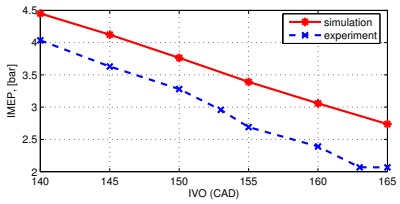

Fig. 5. Experimental and simulated relation between IMEP and IVO.

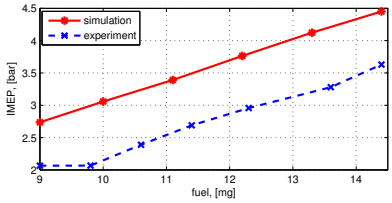

Fig. 6. Experimental and simulated relation between IMEP and the amount of injected fuel.

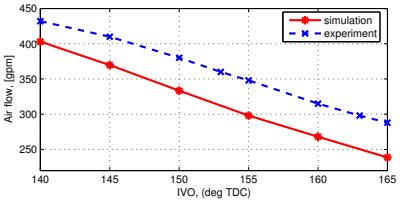

Fig. 7. Experimental and simulated relation between average air flow through the cylinder and IVO.

IV. Control Strategy

We used the proposed engine model to design and test a control structure which can control $IMEP$ and combustion phasing on a cycle-to-cycle basis. After each k-th engine cycle the collected data is processed to calculate the characteristic features of the cycle, $IMEP(k)$ and phasing of 50% mass fraction burned, $MFB(k)$ [19]. These values are then treated as discrete system outputs and used to close the control loop for regulation with respect to desired values, $r(k)_{IMEP}$, $r(k)_{MFB}$.

The experimental and simulation results presented above show a strong evidence that two control inputs, the amount of injected fuel and the IVO can efficiently control operation of the HCCI engine. While the amount of injected fuel controls $IMEP$, the IVO can control combustion phasing by regulating proportion of fresh charge inducted into the cylinder to the amount of exhaust gas trapped from the previous cycle. This control strategy naturally proposes a controller structure represented on Figure 8.

The controller consists of two parallel channels, one for the control of $IMEP$ and another for the control of combustion phasing represented with MFB with the corresponding input channels in fuel and IVO. For the $IMEP$ channel the controller consists of a feedforward term and a feedback term. While the feedforward term is responsible for driving the system from one operating point to another, the feedback term is responsible for stabilizing the system around the current operating point. The feedforward terms are implemented by static maps which transform desired reference signal in $IMEP$ into the system inputs which keep the engine at the desired operating point in steady-state conditions. The feedback terms are PI controllers tuned to stabilize the system with minimal overshoot and oscillations. PI controllers were chosen in order to provide perfect tracking of constant reference inputs, while keeping the control system as simple as possible. Delay blocks are introduced in the reference signals for the feedback channels to account for the fact that at the current cycle k the outputs of the system available for the feedback are those from the previous cycle, $IMEP(k-1)$ and $MFB(k-1)$. The feedforward maps are represented on Figure 9. The PI controllers used for the simulation are:

$$C(z)_{fuel} = \frac{0.04z}{z-1},$$
$$C(z)_{IVO} = \frac{-z}{z-1}.$$

Figure 10 shows the simulation results for the proposed controller and step reference input in $IMEP$ changing from $IMEP = 3\ [bar]$ to $IMEP = 4\ [bar]$, then to $IMEP = 2\ [bar]$ and back to $IMEP = 4\ [bar]$. The first plot of the Figure shows the reference signal and the system response in $IMEP$. Second plot shows the oscillations of the response in MFB around the desired value $MFB = 7\ [deg]$. The last

plot shows deviations of the control inputs from the steady state values of $IVO = 160\ [deg]$ and fuel mass $= 10\ [mg]$. As can be seen from the simulation results, the proposed controller provides good tracking of the reference signal. The step change of 2 $[bar]$ in $IMEP$ is tracked within 3 cycles.

V. Conclusion

In this paper we proposed the model of the two-stroke HCCI engine which described important details of the gas exchange processes taking place in the engine. The concentrations of species in the intake and the exhaust were explicitly modeled. This allows use of the proposed model for implementation of various control strategies. The simulation results obtained with the model showed to have a good fit with the experimental data. Using the proposed model we designed a controller which allowed efficient tracking of $IMEP$ and combustion phasing.

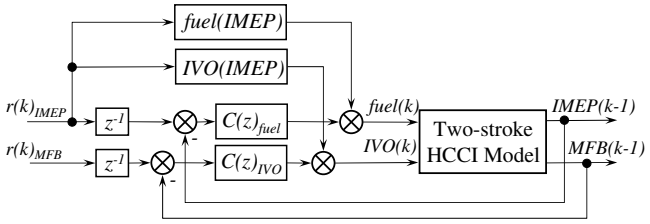

Fig. 8. Control system structure.

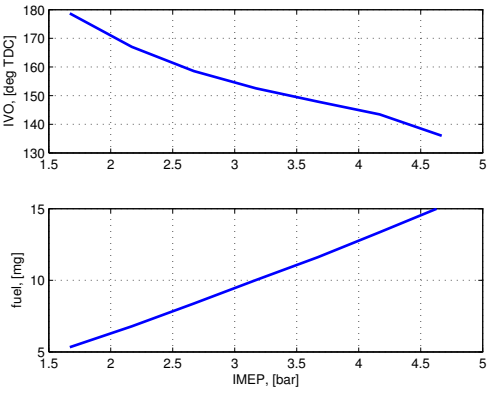

Fig. 9. Feedforward maps between $IMEP$ and IVO, and $IMEP$ and the amount of fuel.

References

[1] Aceves, S.M., Martinez-Frias, J., Flowers, D.L., Smith, J.R., Dibble, R., Wright, J.F., Hessel, R.P. (2001). A decoupled model of detailed fluid mechanics followed by delailed chemical kinetics for prediction of iso-octane HCCI combustion, *SAE 2001-01-3612*.

[2] Bhave, A., Kraft, M., Mauss, F., Oakley, A., & Zhao, H. (2005). Evaluating the EGR-AFR operating range of an HCCI engine. *SAE 2005-01-0161*.

[3] Chiang, C.J., Stefanopoulou, A.G., & Jancović, M. (2007). Nonliner observer-based control of load transitions in homogeneous charge compression ignition engines, *IEEE Trasnaction on Control System Technology*, 15(3), (pp. 438-448).

[4] Chiang, C.J., & Stefanopoulou, A.G. (2006). Sensitivity analysis of combustion timing and duration of homogeneous charge compression ignition (HCCI) engines, *In Proc. of American Control Conference*, (pp. 1857-1862).

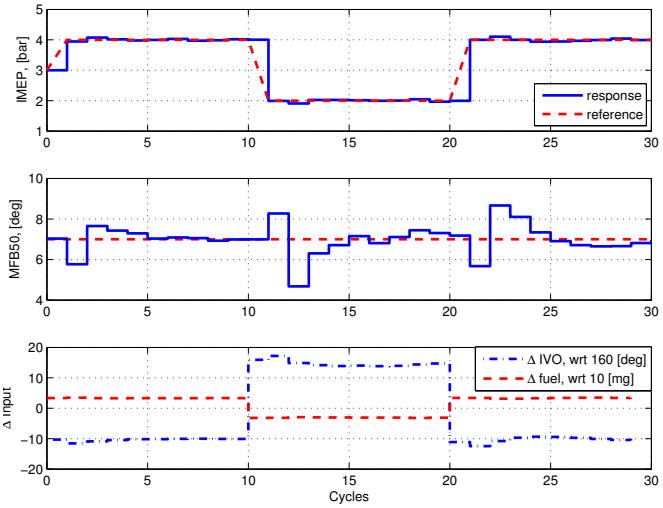

Fig. 10. Step response.

[5] Fiveland, F.B., & Assanis, D.N. A quasi-dimensional HCCI model for performance and emission studies. *In Proc. of the* 9^{th} *Int. Conf. on Numerical Combustion*, No. MS052.

[6] Heywood, J. (1988). Internal combustion engine fundamentals, McGraw-Hill.

[7] Inishi, S., Jo, S.K., Shoda, K., Jo, P.D., & Kato, S. (1979). Active thermo-atmosphere combustion (ATAC) - a new combustion process for internal combustion engines, *SAE 790501*.

[8] Karagiorgis, S., Collings, N., Glover, K., & Petridis, T. (2006). Dynamic modeling of combustion and gas exchange processes for controlled auto-ignition engines. *In Proc. of American Control Conference*, (pp. 1880-1885).

[9] Karrelmeyer, R., Haring, J., Fischer, W., & Hathout, J.P. (2006). Closed-loop control of a 1-cylinder gasoline HCCI engine in dynamic operation, *In Proc. of New Trends in Engine Control, Simulation and Modeling*, (pp. 1-7).

[10] Knierim, K.L. (2007). Modeling and control of HCCI combustion, *Diploma Thesis*, Institute of Applied and Experimental Mechanics, University of Stuttgart.

[11] Kong, S.C., Marriott, C.D., Reitz, R.D., & Christensen, M. (1981). Modeling and experiments of HCCI engine combustion using detailed chemical kinetics with multi-dimensional CFD. *Combustion Science and Technology*, 27, (pp. 31-43).

[12] Koopmans, L., Backlund, O., & Denbratt, I. (2002). Cycle to cycle variations: their influence on cycle resolved gas temperature and unburned hydrocarbons from a camless gasoline compression ignition engine, *SAE 2002-01-0110*

[13] Marriott, C., Kong, S.C., & Reitz, R.D. (2002). Investigation of Hydrocarbon emissions from a direct injection-gasoline premixed charge compression ignited engine, *SAE 2002-01-0419*.

[14] Martinez-Frias, J., Aceves, S.M., Flowers, D., Smith, J.R., & Dibble, R. (2000). HCCI engine control by thermal management, *SAE 2000-01-2869*.

[15] Najt, P.M., & Foster, D.E. (1983). Compression-ignited homogeneous charge combustion, *SAE 830264*

[16] Ogink, A., & Golovitchev, V. (2002). Gasoline HCCI modeling: an engine cycle simulation code with a multi-zone combustion model. *SAE 2002-01-1745*.

[17] Shaver, G.M., Gerdes, J.C., Jain, P., Caton, P.A., & Edwards, C.F. (2003). Modeling for control of HCCI engines. *In Proc. of American Control Conference*, (pp. 749-754).

[18] Shaver, G.M., Roelle, M., & Gerdes, J.C. (2006). A two-input two-output control model of HCCI engines. *In Proc. of American Control Conference*, (pp. 472-477).

[19] Stone, R. (1999). Introduction to internal combustion engunes, SAE International.

[20] Tunestal, P., Olsson, J.O., & Johansson, B. (2001). HCCI operation of a multi-cylinder engine, First Biennial Meeting of the Scandinavian-Nerdic section of the Combustion Institute.